Time-varying formation tracking control for multi-agent systems using distributed multi-sensor multi-target filtering

Jialin Qi[a], Zheng Zhang[a], Xiwang Dong[a,b], Jianglong Yu[a,*], Qingdong Li[a], Hong Jiang[a], Zhang Ren[a]

[a]*School of Automation Science and Electrical Engineering, Science and Technology on Aircraft Control Laboratory, Beihang University, Beijing, 100191, P.R. Chi*
[b]*Institute of Artificial Intelligence, Beihang University, Beijing 100191,*

Abstract

Time-varying formation tracking control problems for multi-agent systems using distributed multi-sensor multi-target filtering are investigated. In order to obtain the accurate state estimations of targets, a distributed multi-sensor multi-target filtering algorithm based on the cubature Kalman filter scheme and multiple heterogeneous sensors is proposed. Then, the state estimations obtained by the filtering algorithm are used to design a time-varying formation tracking protocol for multi-agent systems, enabling these systems to form a time-varying formation and track the convex combination of multiple targets. The estimation errors of filtering algorithm are proved to be bounded by introducing a stochastic process and the boundedness of the formation tracking errors is further proved by using the properties of the Laplacian matrix. Finally, the effectiveness of the proposed algorithm is illustrated by simulation experiments.

Keywords: Time-varying formation, Formation tracking, Distributed multi-sensor multi-target filtering, Cubature Kalman filter

⋆Fully documented templates are available in the elsarticle package on CTAN.

*Corresponding author
Email address: sdjxyjl@buaa.edu.cn (Jianglong Yu)

1. Introduction

The problem of formation tracking has received wide attention from researchers in the past few years [1]-[5] and has played an important rule in military and civil fields [6]-[9]. Formation tracking uses the information interaction between agents and the states of targets to design a protocol, so that the agents can track the targets and keep the desired formation, which is determined by the formation reference [10].

The issue of formation tracking with multi-target has been concerned widely in recent years. The problem of average formation tracking for second-order multi-agent systems with multi-target is investigated in [11], the average state of all targets is tracked by agents. Then [12] proposes a sufficient and necessary condition for achieving time-varying formation tracking for a multi-agent systems with multi-target, and this protocol can be further applied to higher-order systems. The protocol of distributed time-varying formation tracking is proposed in [13]. [14] further considers the fully adaptive time-varying formation tracking problem for high-order nonlinear multi-agent systems with random noise in the dynamics, and the stability and performance of the proposed algorithm are analyzed.

Compared with the centralized filtering, distributed multi-sensor multi-target filtering has the advantages of being real-time, fault-tolerant, and flexible [15], and is divided into two methods by using data association (DA) [16]-[19] and random finite set (RFS) [20]-[23]. The computing speed of distributed filtering with RFS is fast, but the theory of this method is not perfect enough. After associating the data with the method of DA, distributed filtering for nonlinear system is performed through extended Kalman filter (EKF) [24], unscented Kalman filter (UKF) [25] and cubature Kalman filter (CKF) [26]-[28]. Since the weight of each integral point in CKF is same and positive, the numerical stability of CKF is better than UKF. Meanwhile, EKF has lower precision when dealing with second-order nonlinear system compared with CKF [29]. In this case, the problem of distributed multi-sensor multi-target filtering based on the

method of DA and CKF is discussed.

However, in most of the practical scenes, the states of the targets are unknown, i.e., targets are uncooperative. In previous work [30], the authors consider the issue of time-varying formation tracking with unknown disturbances in both agents and targets. In [31], the authors combine the multi-target filtering with formation tracking and propose a formation tracking protocol for heterogeneous second-order system, but they do not consider the case of heterogeneous sensors and nonlinear observation models. The design of formation tracking protocol based on multi-target filtering by multiple heterogeneous sensors with nonlinear observation models is still an important issue that needs to be solved.

In this paper, a distributed multi-target cubature Kalman filter (MT-CKF) algorithm is proposed by assuming that all targets are measured by each sensor, and the results of DA between target measurements and target trajectories are investigated. In this algorithm, radar sensors and infrared sensors are used to observe the targets. The two types of sensors have different measurement capabilities, the radar sensor can measure the distance and angle between the sensor and the target, while the infrared sensor can only measure the angle between the sensor and the target. The estimation errors of MT-CKF algorithm are proved to be bounded. The state estimations obtained from the MT-CKF algorithm are further applied to the problem of formation tracking for multi-agent systems with multi-target, a time-varying formation tracking protocol is proposed and the formation tracking errors are proved to be bounded. The main contributions of this paper are as follows:

1)A distributed MT-CKF algorithm with the nonlinear measuring models based on the CKF scheme and heterogeneous sensors is proposed in this paper. In [31], only linear measuring model is considered. Due to the properties of the sensors in most of the practical scenes, the measuring models are always nonlinear, the approach in [31] cannot be applied to solve the problem in this paper.

2)The estimation errors of the proposed distributed MT-CKF algorithm are proved to be bounded. In [29] and [32], the estimate errors of the CKF scheme

are proved to be bounded, however, only one target is considered, the result in [29] and [32] cannot be extended to deal with the multiple targets problems directly in the current paper.

3)Based on the distributed MT-CKF algorithm, a time-varying formation tracking protocol is proposed and the boundedness of the formation tracking errors is proved. However, in [11]-[14], only the problem that the target states are known by the agents is considered, the approach proposed in [11]-[14] cannot be directly used to solve the issue that targets are uncooperative in this paper.

The rest of this paper is organized as follows. Section 2 defines the communication topology and the system models. Section 3 proposes a distributed MT-CKF algorithm and a time-varying formation tracking protocol. The boundedness of the proposed algorithm is proved in Section 4. Section 5 gives the simulation experiments. This paper is concluded in Section 6.

2. Problem formulation

2.1. Communication topology

The communication structure of the network is described by the directed graphs $G_1 = (V, \varepsilon, \Pi)$ and $G_2 = (D, \chi, W)$, where V and D are the node sets, $\varepsilon \in V \times V$ and $\chi \in D \times D$ are the edge sets, Π and W are the weighted adjacency matrices. The edge $(j, i) \in \varepsilon$ or $(j, i) \in \chi$ means that node i can receive data from node j, and j is the in-neighbor node of i, the in-neighbor set of node i is represented as $\mathrm{N}_i = \{j : (j, i) \in \varepsilon \text{ or } (j, i) \in \chi\}$, $i \notin \mathrm{N}_i$, the number of nodes in set N_i is $|\mathrm{N}_i|$.

Suppose there are M agents, $N-M$ targets, M radar sensors and M_1 infrared sensors in the network, $M \geq M_1$. Let $V_1 = \{1, 2, ..., M\}$, $V_2 = \{M+1, M+2..., N\}$ represent the sets of agents and targets, respectively, $V = V_1 \cup V_2$. Let $D_1 = \{1, 2, ..., M\}$ and $D_2 = \{M+1, M+2, .., M+M_1\}$ represent the sets of radar sensors and infrared sensors, respectively, $D = D_1 \cup D_2$.

Define $\Pi = [\pi_{ij}]_{N \times N}$ as the weighted adjacency matrix with nonnegative elements π_{ij}, which is the corresponding interaction strength of directed edge

(j,i), $j,i \in V$, define π_{ij} as

$$\pi_{ij} = \begin{cases} 0, & i = j \quad or \quad (j,i) \notin \varepsilon \\ b_j > 0, j \in V_2 & and \quad (j,i) \in \varepsilon \\ a_{ij} > 0, j \in V_1 & and \quad (j,i) \in \varepsilon \ , \end{cases} \tag{1}$$

where b_j, a_{ij} can both be taken as 1. Define the in-degree of node i ($i \in V$) as $\deg_{in}(i) = \sum_{j=1}^{N} \pi_{ij}$, then the degree matrix of G_1 is depicted by $DEG = \text{diag}\{\deg_{in}(i), i \in V\}$. Define the Laplacian matrix of G_1 as $L = DEG - \Pi$, then according to (1), one gets $L = \left[\begin{smallmatrix} L_1 & L_2 \\ 0 & 0 \end{smallmatrix} \right]$, where $L_1 \in R^{M \times M}$, $L_2 \in R^{M \times (N-M)}$.

Remark 1: The targets considered in this paper are uncooperative and cannot send their real states to the agents, but the sensors located on the agents can estimate the states of all targets. Therefore, all targets are considered as in-neighbor nodes of the agents and the agents could receive the state estimations from the targets.

2.2. System model

The state dynamic of target s ($s \in V_2$) is modeled as

$$x_{k,s} = \Phi_s x_{k-1,s} + w_{k-1,s} \ , \tag{2}$$

where $x_{k,s} \in R^n$ is the state of the target s at time instant k, $\Phi_s \in R^{n \times n}$ is the system matrix, and $w_{k-1,s} \in R^n$ is the driving Gaussian noise with zero mean and covariance matrix $R_{k-1,s}$.

Define $x_k = [(x_{k,M+1})^T, (x_{k,M+2})^T, ..., (x_{k,N})^T]^T$ as the set of states of all targets at time instant k, the state dynamics of multi-target are modeled as

$$x_k = \bar{\Phi} x_{k-1} + w_{k-1} \ , \tag{3}$$

where $\bar{\Phi} = \text{diag}\{\Phi_{M+1}, \Phi_{M+2}, ..., \Phi_N\}$, $w_{k-1} = [(w_{k-1,M+1})^T, (w_{k-1,M+2})^T, ..., (w_{k-1,N})^T]^T$, w_{k-1} is the driving Gaussian noise with zero mean and covariance matrix $R_{k-1} = \text{diag}\{R_{k-1,M+1}, R_{k-1,M+2}, ..., R_{k-1,N}\}$.

Suppose all sensors are located in M agents, each agent carries one radar sensor and one or zero infrared sensor. The measuring model of sensor i ($i \in D$)

for target s at time instant k is

$$y_{k,s}^{i} = h_{s}^{i}(x_{k,s}) + v_{k,s}^{i} \ , \tag{4}$$

where $y_{k,s}^{i} \in R^{m}$ is the measurement vector for target s, $h_{s}^{i}(\cdot)$ is a continuous differentiable nonlinear measurement function with respect to $x_{k,s}$, $v_{k,s}^{i}$ is the Gaussian measurement noise with zero mean and covariance matrix $Q_{k,s}^{i}$, $h_{s}^{i}(\cdot)$ and $Q_{k,s}^{i}$ are depicted as

$$\begin{cases} h_{s}^{i}(x_{k,s}) = \begin{bmatrix} r_{k,s}^{i} \\ \theta_{k,s}^{i} \end{bmatrix}, Q_{k,s}^{i} = \begin{bmatrix} C_{k,s}^{i,r} & 0 \\ 0 & C_{k,s}^{i,\theta} \end{bmatrix}, i \in D_{1} \\ h_{s}^{i}(x_{k,s}) = [\theta_{k,s}^{i}], Q_{k,s}^{i} = C_{k,s}^{i,\theta}, i \in D_{2} \ , \end{cases} \tag{5}$$

where $r_{k,s}^{i}$ and $\theta_{k,s}^{i}$ are the radial distance and angle between target s and sensor i at time instant k, respectively. $C_{k,s}^{i,r}$ and $C_{k,s}^{i,\theta}$ are the measurement noise covariances of the radial distance and the angle of i, respectively. The distance measurement of the radar sensor i' located in the same agent with the infrared sensor i is used to expand the dimension of $y_{k,s}^{i}$, then the measuring model for target s by sensor i ($i \in D$) at time instant k is

$$\begin{aligned} &\bar{y}_{k,s}^{i} = \bar{h}_{s}^{i}(x_{k,s}) + \bar{v}_{k,s}^{i}, \\ &\begin{cases} \bar{h}_{s}^{i}(x_{k,s}) = \begin{bmatrix} r_{k,s}^{i} \\ \theta_{k,s}^{i} \end{bmatrix}, \bar{Q}_{k,s}^{i} = \begin{bmatrix} C_{k,s}^{i,r} & 0 \\ 0 & C_{k,s}^{i,\theta} \end{bmatrix}, i \in D_{1} \\ \bar{h}_{s}^{i}(x_{k,s}) = \begin{bmatrix} r_{k,s}^{i'} \\ \theta_{k,s}^{i} \end{bmatrix}, \bar{Q}_{k,s}^{i} = \begin{bmatrix} C_{k,s}^{i',r} & 0 \\ 0 & C_{k,s}^{i,\theta} \end{bmatrix}, i \in D_{2} \ , \end{cases} \end{aligned} \tag{6}$$

where $\bar{v}_{k,s}^{i}$ is the Gaussian measurement noise with zero mean and covariance matrix $\bar{Q}_{k,s}^{i}$. (6) is used as the measuring model of the sensor network in the filtering algorithm. Since $h_{s}^{i}(\cdot)$ is a continuous differentiable function with respect to $x_{k,s}$, then $\bar{h}_{s}^{i}(\cdot)$ obtained by (6) is also a continuous differentiable function with respect to $x_{k,s}$.

Define $y_{k}^{i} = [(\bar{y}_{k,M+1}^{i})^{T}, (\bar{y}_{k,M+2}^{i})^{T}, ..., (\bar{y}_{k,N}^{i})^{T}]^{T}$ as the measurement of sensor i ($i \in D$) for targets s ($s \in V_{2}$) at time instant k. Then the measuring model of sensor i for multi-target is

$$y_{k}^{i} = h^{i}(x_{k}) + v_{k}^{i} \ , \tag{7}$$

where $h^i(x_k) = [(\bar{h}_s^i(x_{k,M+1}))^T, (\bar{h}_s^i(x_{k,M+2}))^T, ..., (\bar{h}_s^i(x_{k,N}))^T]^T$, $v_k^i = [(\bar{v}_{k,M+1}^i)^T, (\bar{v}_{k,M+2}^i)^T, ..., (\bar{v}_{k,N}^i)^T]^T$, v_k^i is the Gaussian measurement noise with zero mean and covariance matrix $Q_k^i = \text{diag}\{\bar{Q}_{k,M+1}^i, \bar{Q}_{k,M+2}^i, ..., \bar{Q}_{k,N}^i\}$.

3. Formation tracking based on distributed MT-CKF algorithm

3.1. Distributed MT-CKF algorithm

1) Initialize

For each sensor node i ($i \in D$), initialize the state estimation $\hat{x}_0^i$ and error covariance matrix P_0^i at time instant $k = 0$ according to (8) and (9),

$$\hat{x}_0^i = E(x_0) \ , \tag{8}$$

$$P_0^i = E[(x_0 - \hat{x}_0^i)(x_0 - \hat{x}_0^i)^T] \ . \tag{9}$$

2) Predict

By using the Cholesky decomposition approach for P_{k-1}^i, one gets S_{k-1}^i according to (10)

$$P_{k-1}^i = S_{k-1}^i (S_{k-1}^i)^T \ . \tag{10}$$

Based on the decomposition results, the cubature points are calculated as

$$x_{k-1}^{i,e} = S_{k-1}^i [(\xi_{M+1}^e)^T, (\xi_{M+2}^e)^T, ..., (\xi_N^e)^T]^T + \hat{x}_{k-1}^i \ , \tag{11}$$

where $e = 1, 2, ..., 2n$, ξ_s^e ($s \in V_2$) is the eth element of ξ_s,

$$\xi_s = \sqrt{n} \underbrace{\left\{ \begin{bmatrix} 1 \\ 0 \\ \vdots \\ 0 \end{bmatrix}, \begin{bmatrix} 0 \\ 1 \\ \vdots \\ 0 \end{bmatrix}, ..., \begin{bmatrix} 0 \\ 0 \\ \vdots \\ 1 \end{bmatrix}, \begin{bmatrix} -1 \\ 0 \\ \vdots \\ 0 \end{bmatrix}, \begin{bmatrix} 0 \\ -1 \\ \vdots \\ 0 \end{bmatrix}, ..., \begin{bmatrix} 0 \\ 0 \\ \vdots \\ -1 \end{bmatrix} \right\}}_{2n} \ .$$

Then the propagated cubature points are calculated by

$$x_{k|k-1}^{i,e} = \bar{\Phi} x_{k-1}^{i,e} \ . \tag{12}$$

The priori state estimation $\hat{x}^i_{k|k-1}$ and priori estimation error covariance matrix $P^i_{k|k-1}$ are obtained by

$$\hat{x}^i_{k|k-1} = \frac{1}{2n}\sum_{e=1}^{2n} x^{i,e}_{k|k-1} \ , \tag{13}$$

$$\begin{aligned}
\tilde{P}^i_{k|k-1} &= \tfrac{1}{2n}\sum_{e=1}^{2n} x^{i,e}_{k|k-1}\left(x^{i,e}_{k|k-1}\right)^T - \hat{x}^i_{k|k-1}\left(\hat{x}^i_{k|k-1}\right)^T + R_{k-1} \\
&= \begin{bmatrix} \tilde{P}^{i,[1,1]}_{k|k-1} & ,\dots, & \tilde{P}^{i,[1,N-M]}_{k|k-1} \\ \vdots & ,\ddots, & \vdots \\ \tilde{P}^{i,[N-M,1]}_{k|k-1} & ,\dots, & \tilde{P}^{i,[N-M,N-M]}_{k|k-1} \end{bmatrix} , \\
P^i_{k|k-1} &= \mathrm{diag}\{\tilde{P}^{i,[1,1]}_{k|k-1}, \tilde{P}^{i,[2,2]}_{k|k-1}, ..., \tilde{P}^{i,[N-M,N-M]}_{k|k-1}\} \ .
\end{aligned} \tag{14}$$

3) Update

The obtained cubature points are transformed into

$$y^{i,e}_{k|k-1} = h^i(x^{i,e}_{k-1}), e = 1, 2, ..., 2n \ . \tag{15}$$

Then the prediction of measurement $\hat{y}^i_k$ and error covariance $P^i_{k|k-1,yy}$, $P^i_{k|k-1,xy}$ are obtained by

$$\hat{y}^i_k = \frac{1}{2n}\sum_{e=1}^{2n} y^{i,e}_{k|k-1} \ , \tag{16}$$

$$\begin{aligned}
\tilde{P}^i_{k|k-1,yy} &= \tfrac{1}{2n}\sum_{e=1}^{2n} y^{i,e}_{k|k-1}\left(y^{i,e}_{k|k-1}\right)^T - \hat{y}^i_k\left(\hat{y}^i_k\right)^T + Q^i_k \\
&= \begin{bmatrix} \tilde{P}^{i,[1,1]}_{k|k-1,yy} & ,\dots, & \tilde{P}^{i,[1,N-M]}_{k|k-1,yy} \\ \vdots & ,\ddots, & \vdots \\ \tilde{P}^{i,[N-M,1]}_{k|k-1,yy} & ,\dots, & \tilde{P}^{i,[N-M,N-M]}_{k|k-1,yy} \end{bmatrix} , \\
P^i_{k|k-1,yy} &= \mathrm{diag}\{\tilde{P}^{i,[1,1]}_{k|k-1,yy}, \tilde{P}^{i,[2,2]}_{k|k-1,yy}, ..., \tilde{P}^{i,[N-M,N-M]}_{k|k-1,yy}\} \ .
\end{aligned} \tag{17}$$

$$\begin{aligned}
\tilde{P}^i_{k|k-1,xy} &= \tfrac{1}{2n}\sum_{e=1}^{2n} x^{i,e}_{k-1}\left(y^{i,e}_{k|k-1}\right)^T - \hat{x}^i_{k|k-1}\left(\hat{y}^i_k\right)^T \\
&= \begin{bmatrix} \tilde{P}^{i,[1,1]}_{k|k-1,xy} & ,\dots, & \tilde{P}^{i,[1,N-M]}_{k|k-1,xy} \\ \vdots & ,\ddots, & \vdots \\ \tilde{P}^{i,[N-M,1]}_{k|k-1,xy} & ,\dots, & \tilde{P}^{i,[N-M,N-M]}_{k|k-1,xy} \end{bmatrix} , \\
P^i_{k|k-1,xy} &= \mathrm{diag}\{\tilde{P}^{i,[1,1]}_{k|k-1,xy}, \tilde{P}^{i,[2,2]}_{k|k-1,xy}, ..., \tilde{P}^{i,[N-M,N-M]}_{k|k-1,xy}\} \ .
\end{aligned} \tag{18}$$

The filter gain is

$$K^i_k = P^i_{k|k-1,xy}(P^i_{k|k-1,yy})^{-1} \ . \tag{19}$$

The state estimation and error covariance of all targets at time instant k are calculated as

$$\hat{x}_k^i = \hat{x}_{k|k-1}^i + K_k^i(y_k^i - \hat{y}_k^i) \ , \tag{20}$$

$$P_k^i = P_{k|k-1}^i - K_k^i P_{k|k-1,yy}^i (K_k^i)^T \ . \tag{21}$$

4) Consensus iterative

Assumption 1: The directed interaction topology of muti-agent systems is strongly connected, and the sensor located on the agent can receive data from other sensors located on the same agent and the in-neighbor agents. The consensus weights w_{ij} are chosen to make sure that the consensus matrix W is doubly stochastic.

As we know in [33], W is doubly stochastic if the sum of the elements in each row and column of W is 1. In order to make sure that W is doubly stochastic, the elements of W are chosen according to the Metropolis weights principle as

$$w_{ij} = \begin{cases} \frac{1}{1+\max(|\mathrm{N}_i|,|\mathrm{N}_j|)}, \ if \ i \in D, j \in N_i \\ 1 - \sum\limits_{j \in N_i} w_{ij}, \ if \ i \in D, i = j \\ 0, \ if \ i,j \in D, j \notin N_i \ . \end{cases} \tag{22}$$

Suppose l ($l = 1, 2, ..., L$) is the lth consensus step, $\hat{x}_k^{i,l}$ and $P_k^{i,l}$ are the state estimation and error covariance obtained by sensor i at time instant k after the lth iteration, respectively. Initialize $\hat{x}_k^{i,l}$, $P_k^{i,l}$ as $\hat{x}_k^{i,0} = \hat{x}_k^i$, $P_k^{i,0} = P_k^i$ when $l = 0$. Then $\hat{x}_k^{i,l}$ and $P_k^{i,l}$ are obtained by the following consensus strategy

$$\hat{x}_k^{i,l} = w_{ii}\hat{x}_k^{i,l-1} + \sum_{j \in N_i} w_{ij}\hat{x}_k^{j,l-1} \ , \tag{23}$$

$$P_k^{i,l} = w_{ii}P_k^{i,l-1} + \sum_{j \in N_i} w_{ij}P_k^{j,l-1} \ . \tag{24}$$

After a total of L iterations, sensor i gets $\hat{x}_k^i = \hat{x}_k^{i,L} = [(\hat{x}_{k,M+1}^{i,L})^T, (\hat{x}_{k,M+2}^{i,L})^T, ..., (\hat{x}_{k,N}^{i,L})^T]^T$, $P_k^i = P_k^{i,L} = \mathrm{diag}(P_{k,M+1}^{i,L}, P_{k,M+2}^{i,L}, ..., P_{k,N}^{i,L})$, where $\hat{x}_{k,s}^{i,L}$ and $P_{k,s}^{i,L}$ are the state estimation and error covariance of target s ($s \in V_2$) after L iterations at time instant k, respectively.

When Assumption 1 holds, all elements in $\lim_{L \to +\infty} W^L$ converge to $1/|D|$. According to the fusion rule, after $L \to +\infty$ iterations, the state estimations

and error covariances are achieved to be converge, i.e. for $\forall i, j \in D$, one gets $\hat{x}_k = \hat{x}_k^{i,L} = \hat{x}_k^{j,L} = [(\hat{x}_{k,M+1})^T, (\hat{x}_{k,M+2})^T, ..., (\hat{x}_{k,N})^T]^T$, $P_k = P_k^{i,L} = P_k^{j,L} = \text{diag}(P_{k,M+1}, P_{k,M+2}..., P_{k,N})$ when $L \to +\infty$, where $\hat{x}_{k,s}$ and $P_{k,s}$ are the state estimation and error covariance of target s ($s \in V_2$) after $L \to +\infty$ iterations at time instant k, respectively.

Algorithm 1 in Table 1 summarizes the distributed MT-CKF algorithm proposed in this paper.

Table 1 - Distributed MT-CKF algorithm

Algorithm 1 Distributed MT-CKF algorithm

1) Initialization:

$x_k = \bar{\Phi} x_{k-1} + w_{k-1}$,

$y_k^i = h^i(x_k) + v_k^i$.

2) Predict:

$\hat{x}_{k|k-1}^i = \frac{1}{2n} \sum_{e=1}^{2n} x_{k|k-1,g}^i$,

$P_{k|k-1}^i = \text{diag}\{\tilde{P}_{k|k-1}^{i,[1,1]}, \tilde{P}_{k|k-1}^{i,[2,2]}, ..., \tilde{P}_{k|k-1}^{i,[N-M,N-M]}\}$.

3) Update:

$P_{k|k-1,yy}^i = \text{diag}\{\tilde{P}_{k|k-1,yy}^{i,[1,1]}, \tilde{P}_{k|k-1,yy}^{i,[2,2]}, ..., \tilde{P}_{k|k-1,yy}^{i,[N-M,N-M]}\}$,

$P_{k|k-1,xy}^i = \text{diag}\{\tilde{P}_{k|k-1,xy}^{i,[11]}, \tilde{P}_{k|k-1,xy}^{i,[2,2]}, ..., \tilde{P}_{k|k-1,xy}^{i,[N-M,N-M]}\}$,

$K_k^i = P_{k|k-1,xy}^i (P_{k|k-1,yy}^i)^{-1}$,

$\hat{x}_k^i = \hat{x}_{k|k-1}^i + K_k^i (y_k^i - \hat{y}_k^i)$,

$P_k^i = P_{k|k-1}^i - K_k^i P_{k|k-1,yy}^i (K_k^i)^T$.

4) Consensus iterative:

A) Initialize:

$\hat{x}_k^{i,0} = \hat{x}_k^i$,$P_k^{i,0} = P_k^i$.

B) Choose the consensus matrix as (22)

for $\quad l = 1, 2, ..., L$

Exchange information with neighbor nodes and calculate the weighted fused state estimation and error covariance:

$\hat{x}_k^{i,l} = w_{ii} \hat{x}_k^{i,l-1} + \sum_{j \in N_i} w_{ij} \hat{x}_k^{j,l-1}$,

$P_k^{i,l} = w_{ii} P_k^{i,l-1} + \sum_{j \in N_i} w_{ij} P_k^{j,l-1}$.

end

5) The state estimation and error covariance of target s ($s \in V_2$) are obtained by

$\hat{x}_k^i = \hat{x}_k^{i,L} = [(\hat{x}_{k,M+1}^{i,L})^T, (\hat{x}_{k,M+2}^{i,L})^T, ..., (\hat{x}_{k,N}^{i,L})^T]^T$,

$P_k^i = P_k^{i,L} = \mathrm{diag}(P_{k,M+1}^{i,L}, P_{k,M+2}^{i,L}, ..., P_{k,N}^{i,L})$.

3.2. Time-varying formation tracking based on distributed MT-CKF algorithm

Suppose $\Phi_s = \Phi$ ($s \in V_2$) in (2), then the state dynamic of target s ($s \in V_2$) are shown in (25).

$$x_{k,s} = \Phi x_{k-1,s} + w_{k-1,s} \ . \tag{25}$$

After using the MT-CKF algorithm with $L \to +\infty$ iterations, the state estimation for target $s \in V_2$ at time instant $k-1$ is $\hat{x}_{k-1,s}$, and the state dynamics of the agents are depicted as

$$X_k^c = \Phi X_{k-1}^c + B u_{k-1}^c, c \in V_1 \ , \tag{26}$$

where $X_k^c \in R^n$ is the state of agent c at time instant k, $u_{k-1}^c \in R^r$ is the time-varying formation tracking protocol of c. Note that $B \in R^{n\times r}$ and $rank(B) = r$, there exists a nonsingular matrix $T = [\tilde{B}^T, \bar{B}^T]^T$ consisted of $\tilde{B} \in R^{r\times n}$ and $\bar{B} \in R^{(n-r)\times n}$, where $\tilde{B}B = I_r$, $\bar{B}B = 0$, I_r is an unit matrix of size r. u_{k-1}^c is defined as

$$\begin{aligned} u_{k-1}^c = \ & K \sum_{j=1}^{M} \pi_{cj}((X_{k-1}^c - g_{k-1}^c) - (X_{k-1}^j - g_{k-1}^j)) \\ & + K \sum_{s=M+1}^{N} \pi_{cs}(X_{k-1}^c - g_{k-1}^c - \hat{x}_{k-1,s}) + n_{k-1}^c \ , \end{aligned} \tag{27}$$

where $c \in V_1$, $n_{k-1}^c = -\tilde{B}(\Phi g_{k-1}^c - g_k^c) \in R^r$ is the formation tracking compensational signal. $g_{k-1}^c \in R^n$ is the relative state of agent c at time instant $k-1$ corresponding to the formation reference $\sum_{s=M+1}^{N} \alpha_s \hat{x}_{k-1,s}$, which is the convex combination of the state estimations of all targets at time instant $k-1$, $\alpha_s, s \in V_2$ is a positive constant satisfying $\sum_{s=M+1}^{N} \alpha_s = 1$.

4. Convergence analysis

In this section, the convergence properties of the proposed time-varying formation tracking control algorithm for multi-agent systems using distributed

multi-sensor multi-target filtering are analyzed.

Expanding (6) using Taylor series and introducing matrix $\beta_{k,s}^i$ to compensate for the errors arising from ignoring higher order terms yield $\bar{y}_{k,s}^i = \beta_{k,s}^i H_{k,s}^i x_{k,s} + \bar{v}_{k,s}^i$, where $H_{k,s}^i = \frac{\partial \bar{h}_s^i(x)}{\partial x}\Big|_{x=x_{k,s}}$.

Assumption 2. There exist $\underline{\phi}, \bar{\phi}, \underline{\beta}, \bar{\beta}, \underline{h}, \bar{h} \neq 0$ such that the following inequalities hold when $k \geq 0$:

$$\begin{aligned}
&\underline{\phi}^2 I_n \leq \Phi_s \left(\Phi_s\right)^T \leq \bar{\phi}^2 I_n \ , \\
&\underline{\beta}^2 I_m \leq \beta_{k,s}^i \left(\beta_{k,s}^i\right)^T \leq \bar{\beta}^2 I_m \ , \\
&\underline{h}^2 I_m \leq H_{k,s}^i \left(H_{k,s}^i\right)^T \leq \bar{h}^2 I_m, i \in D, s \in V_2 \ .
\end{aligned}$$

Assumption 3. There exist real numbers $p_{\min}, p_{\max}, \underline{p}, \bar{p}, \underline{q}, \bar{q}, \underline{r}, \bar{r} > 0$ such that the following inequalities hold:

$$\begin{aligned}
&p_{\min} \leq p^i \leq p_{\max}, \\
&\underline{p}_n \leq P_{k,s} \leq \bar{p} I_n, \\
&\underline{q}_m \leq \bar{Q}_{k,s}^i \leq \bar{q} I_m, \\
&\underline{r}_n \leq R_{k,s} \leq \bar{r} I_n, i \in D, s \in V_2,
\end{aligned}$$

where $p = [p^1, ..., p^{M+M_1}]$ is the Perron-Frobenius left eigenvector of the matrix W^L.

Remark 2: Assumptions 2-3 are applied widely to deal with the stochastic stability of the estimation error of CKF (see [29], [34]-[35]).

Lemma 1 ([34]): For any given $x, y \in R^n$, and scalar $\delta > 0$, one has $xy^T + yx^T \leq \delta x x^T + \delta^{-1} y y^T$.

Lemma 2 ([12]): If Assumption 1 is satisfied, all eigenvalues of L_1 have positive real parts and every row of matrix $-L_1^{-1} L_2$ is equal to $[b_{M+1}, b_{M+2}, ..., b_N] / \sum_{j=M+1}^{N} b_j$.

Theorem 1: Under the conditions of Assumptions 1-3, the state estimation error $\tilde{x}_k = x_k - \hat{x}_k$ obtained by the MT-CKF filtering algorithm satisfies $E(\| \tilde{x}_k \|^2) \leq \sigma$, where σ is a constant value, and $E(\| w_{k-1} \|^2)$ is also bounded.

Proof: $\tilde{x}_{k,s} = x_{k,s} - \hat{x}_{k,s}$ and $w_{k-1,s}$, $s \in V_2$ are proved to be bounded in mean square in [29] and [32] by introducing a stochastic process, i.e. $E(\|$

$\tilde{x}_{k,s}\|^2) \leq \sigma_s$, $E(\| w_{k-1,s}\|^2) \leq \vartheta_s$, where σ_s and ϑ_s are constant values, then one gets

$$\begin{aligned} & E(\| \hat{x}_k - x_k\|^2) \\ & = E(\| [(\hat{x}_{k,M+1} - x_{k,M+1})^T, ..., (\hat{x}_{k,N} - x_{k,N})^T]^T\|^2) \\ & = E(\| \hat{x}_{k,M+1} - x_{k,M+1}\|^2) + ... + E(\| \hat{x}_{k,N} - x_{k,N}\|^2) \\ & \leq \sigma_{M+1} + ... + \sigma_N \\ & = \sigma \ . \end{aligned} \tag{28}$$

Similar procedure is followed to prove that $E(\| w_{k-1}\|^2)$ is also bounded.

Remark 3: In Theorem 1, the boundedness of Algorithm 1 is proved. The distributed MT-CKF algorithm proposed in this paper has large generality. If $N - M = 1$, this algorithm is capable to tackle the filtering issues with one target in [29] and [32], which proved the boundedness of the estimate errors for only one target.

Define that multi-agent systems are able to achieve time-varying formation tracking with multi-target when the formation tracking errors satisfy the condition that $\lim_{k\to+\infty} E\left(\left\|X_k^c - g_k^c - \sum_{s=M+1}^{N} \alpha_s x_{k,s}\right\|^2\right)$, $c \in V_1$ are bounded.

Theorem 2: If $\Phi + \lambda_c BK$ $(c \in V_1)$ is Schur stable and the condition $\lim\limits_{k\to+\infty} (\bar{B}\Phi g_{k-1}^c - \bar{B} g_k^c) = 0$ is satisfied, the multi-agent systems with multi-target can achieve time-varying formation tracking under the protocol (27) and the state estimation of all targets acquired from Algorithm 1.

Proof: Define $X_k = [(X_k^1)^T, (X_k^2)^T, ..., (X_k^M)^T]^T$, $u_k = [(u_k^1)^T, (u_k^2)^T, ..., (u_k^M)^T]^T$, $n_k = [(n_k^1)^T, (n_k^2)^T, ..., (n_k^M)^T]^T$, $g_k = [(g_k^1)^T, (g_k^2)^T, ..., (g_k^M)^T]^T$. When u_{k-1}^c is taken as equation (27), (25) and (26) are expressed as

$$x_k = (I_{N-M} \otimes \Phi) x_{k-1} + w_{k-1} = \bar{\Phi} x_{k-1} + w_{k-1} \ , \tag{29}$$

$$\begin{aligned} X_k = \ & (I_M \otimes \Phi + L_1 \otimes BK) X_{k-1} + (I_M \otimes B) n_{k-1} \\ & + (L_2 \otimes BK) \hat{x}_{k-1} - (L_1 \otimes BK) g_{k-1} \ . \end{aligned} \tag{30}$$

where $\otimes$ represents the Kronecker product. Suppose $\theta_k^c = X_k^c - g_k^c, c \in V_1$, define $\theta_k = [(\theta_k^1)^T, (\theta_k^2)^T, ..., (\theta_k^M)^T]^T$, then (30) is expressed as

$$\begin{aligned} \theta_k = \ & (I_M \otimes \Phi + L_1 \otimes BK) \theta_{k-1} + (I_M \otimes \Phi) g_{k-1} \\ & - (I_M \otimes I_n) g_k + (I_M \otimes B) n_{k-1} + (L_2 \otimes BK) \hat{x}_{k-1} \ . \end{aligned} \tag{31}$$

Suppose $\phi_k^c = \sum_{j=1}^{M} \pi_{cj}(\theta_k^c - \theta_k^j) + \sum_{s=M+1}^{N} \pi_{cs}(\theta_k^c - \hat{x}_{k,s})$, $c \in V_1$, define $\phi_k = [(\phi_k^1)^T, (\phi_k^2)^T, ..., (\phi_k^M)^T]^T$, one gets

$$\phi_k = (L_1 \otimes I_n)\theta_k + (L_2 \otimes I_n)\hat{x}_k \ . \tag{32}$$

According to (32), one has

$$\theta_{k-1} = (L_1^{-1} \otimes I_n)\phi_{k-1} - (L_1^{-1}L_2 \otimes I_n)\hat{x}_{k-1} \ . \tag{33}$$

Substituting (31), (33) into (32) yields

$$\begin{aligned} \phi_k = \ & (I_M \otimes \Phi + L_1 \otimes BK)\phi_{k-1} + (L_1 \otimes \Phi)g_{k-1} - (L_1 \otimes I_n)g_k \\ & + (L_1 \otimes B)n_{k-1} + (L_2 \otimes I_n)\hat{x}_k - (L_2 \otimes \Phi)\hat{x}_{k-1} \ . \end{aligned} \tag{34}$$

Define $\bar{\phi}_k = (U^{-1} \otimes I_n)\phi_k$. Then (34) can be transformed into (35), where $U \in C^{M \times M}$ is a nonsingular matrix satisfying $U^{-1}L_1U = J$, J is the Jordan canonical form of L_1. The diagonal elements λ_c ($c \in V_1$) of J satisfy $\mathrm{Re}(\lambda_1) \leq \mathrm{Re}(\lambda_2) \leq \cdots \leq \mathrm{Re}(\lambda_M)$.

$$\begin{aligned} \bar{\phi}_k = \ & (I_M \otimes \Phi + J \otimes BK)\bar{\phi}_{k-1} + (U^{-1}L_1 \otimes \Phi)g_{k-1} \\ & - (U^{-1}L_1 \otimes I_n)g_k + (U^{-1}L_1 \otimes B)n_{k-1} \\ & + (U^{-1}L_2 \otimes I_n)\hat{x}_k - (U^{-1}L_2 \otimes \Phi)\hat{x}_{k-1} \ . \end{aligned} \tag{35}$$

According to $\lim_{k \to +\infty}(\bar{B}\Phi g_{k-1}^c - \bar{B}g_k^c) = 0$, it is proved that

$$\lim_{k \to +\infty}(\bar{B}\Phi g_{k-1}^c - \bar{B}g_k^c + \bar{B}Bn_{k-1}^c) = 0 \ . \tag{36}$$

According to $n_{k-1}^c = -\tilde{B}(\Phi g_{k-1}^c - g_k^c)$, it is proved that

$$\tilde{B}\Phi g_{k-1}^c - \tilde{B}g_k^c + \tilde{B}Bn_{k-1}^c = 0 \ . \tag{37}$$

According to (36), (37) and $T = [\tilde{B}^T, \bar{B}^T]^T$ is a nonsingular matrix, one gets

$$\lim_{k \to +\infty}(\Phi g_{k-1}^c - g_k^c + Bn_{k-1}^c) = 0 \ .$$

Then it can be obtained that

$$\lim_{k \to +\infty}((I_M \otimes \Phi)g_{k-1} - (I_M \otimes I_n)g_k + (I_M \otimes B)n_{k-1}) = 0 \ . \tag{38}$$

By multiplying $U^{-1}L_1 \otimes I_n$ on both sides of (38), one gets

$$\lim_{k\to+\infty}((U^{-1}L_1 \otimes \Phi)g_{k-1} - (U^{-1}L_1 \otimes I_n)g_k + (U^{-1}L_1 \otimes B)n_{k-1}) = 0\ . \quad (39)$$

For $s \in D$, according to (30), one has

$$\begin{aligned}
& E(\parallel (U^{-1}L_2 \otimes I_n)\hat{x}_k - (U^{-1}L_2 \otimes \Phi)\hat{x}_{k-1}\parallel^2) \\
\leq\ & E(\parallel U^{-1}L_2 \otimes I_n\parallel^2 \parallel (I_{N-M} \otimes I_n)\hat{x}_k - (I_{N-M} \otimes \Phi)\hat{x}_{k-1}\parallel^2) \\
=\ & E(\parallel U^{-1}L_2 \otimes I_n\parallel^2)E(\parallel \hat{x}_k - \bar{\Phi}\hat{x}_{k-1}\parallel^2) \\
=\ & E(\parallel U^{-1}L_2 \otimes I_n\parallel^2)E(\parallel \hat{x}_k - x_k + \bar{\Phi}x_{k-1} + w_{k-1} - \bar{\Phi}\hat{x}_{k-1}\parallel^2) \quad (40) \\
\leq\ & E(\parallel U^{-1}L_2 \otimes I_n\parallel^2)E(\parallel \hat{x}_k - x_k\parallel^2 + \parallel \bar{\Phi}(x_{k-1} - \hat{x}_{k-1})\parallel^2 \\
& + \parallel w_{k-1}\parallel^2 + 2 \parallel \hat{x}_k - x_k \parallel\parallel \bar{\Phi}(x_{k-1} - \hat{x}_{k-1}) \parallel \\
& +2 \parallel \bar{\Phi}(x_{k-1} - \hat{x}_{k-1}) \parallel\parallel w_{k-1} \parallel +2 \parallel \hat{x}_k - x_k \parallel\parallel w_{k-1} \parallel)\ .
\end{aligned}$$

By applying Lemma 1 to (40), the following inequailty holds

$$\begin{aligned}
& E(\parallel (U^{-1}L_2 \otimes I_n)\hat{x}_k - (U^{-1}L_2 \otimes \Phi)\hat{x}_{k-1}\parallel^2) \\
\leq\ & E(\parallel U^{-1}L_2 \otimes I_n\parallel^2)[\eta_1 E(\parallel \hat{x}_k - x_k\parallel^2) \quad (41) \\
& +\eta_2 E(\parallel \bar{\Phi}(x_{k-1} - \hat{x}_{k-1})\parallel^2) + \eta_3 E(\parallel w_{k-1}\parallel^2)]\ ,
\end{aligned}$$

where $\eta_1 = 1 + \delta_1 + \delta_2$, $\eta_2 = 1 + \delta_1^{-1} + \delta_3$, $\eta_3 = 1 + \delta_2^{-1} + \delta_3^{-1}$, and δ_1, δ_2, δ_3 are all positive scalars.

According to Theorem 1, $E(\parallel \hat{x}_k - x_k\parallel^2)$ and $E(\parallel w_{k-1}\parallel^2)$ are bounded, then $E(\parallel (U^{-1}L_2 \otimes I_n)\hat{x}_k - (U^{-1}L_2 \otimes \Phi)\hat{x}_{k-1}\parallel^2)$ is bounded. From the structure of J, one gets that if $\Phi + \lambda_c BK$ is Schur stable, then $I_M \otimes \Phi + J \otimes BK$ is also Schur stable. It can be obtained that $E(\parallel \bar{\phi}_k\parallel^2)$ must be bounded, which means $E(\parallel (U^{-1} \otimes I_n)\phi_k\parallel^2)$ is bounded. Therefore, $E(\parallel \phi_k\parallel^2)$ is bounded. Combining with (32), one gets that $\lim_{k\to+\infty} E(\parallel X_k - g_k - (-L_1^{-1}L_2 \otimes I_n)\hat{x}_k\parallel^2)$ is bounded. According to Lemma 2, one gets that $\lim_{k\to+\infty} E(\parallel X_k^c - g_k^c - \sum_{s=M+1}^{N}(\frac{b_s}{\sum_{j=M+1}^{N} b_j}$ $\hat{x}_{k,s})\parallel^2)$ is bounded, i.e. the multi-agent systems can achieve time-varying formation tracking with multi-target. The errors of formation tracking are increasing with the state estimation errors of multi-target and the errors generated in modeling the state dynamics of multi-target.

5. Numerical simulation

In this section, the effectiveness of the time-varying formation tracking control for multi-agent systems using distributed MT-CKF algorithm is illustrated. A practical scenario involving multiple uncooperative targets is utilized here to justify the potential applicability of the proposed algorithm.

Consider the case of the multi-agent systems with 10 agents, and there are 3 targets need to be tracked. The state of target s at time instant k is expressed as $x_{k,s} = [a_{k,s}, b_{k,s}, \dot{a}_{k,s}, \dot{b}_{k,s}]^T$, $s = \{M+1, M+2, M+3\}$, $k \in [1, 100]$, where $a_{k,s}$, $b_{k,s}$ are the position of s in direction X and direction Y, respectively, $\dot{a}_{k,s}$ and $\dot{b}_{k,s}$ are the velocity of s in direction X and direction Y, respectively. The state dynamics of target s is modeled as (2), where

$$\Phi_s = \Phi = \begin{bmatrix} 1 & 0 & \sin(\omega*T)/\omega & -(1-\cos(\omega*T)/\omega \\ 0 & 1 & (1-\cos(\omega*T)/\omega & -\sin(\omega*T)/\omega \\ 0 & 0 & \cos(\omega*T) & -\sin(\omega*T) \\ 0 & 0 & \sin(\omega*T) & \sin(\omega*T) \end{bmatrix},$$

$\omega = -\frac{3\pi}{180}$, T=1 is the sensing period, $R_{k-1,s}$=$0.05I_4$. The trajectories of the targets with initial states $[-200, -200, 10, 10]^T$, $[-200, -210, 10, 10]^T$, $[-200, -220, 10, 10]^T$ are shown in Fig. 1.

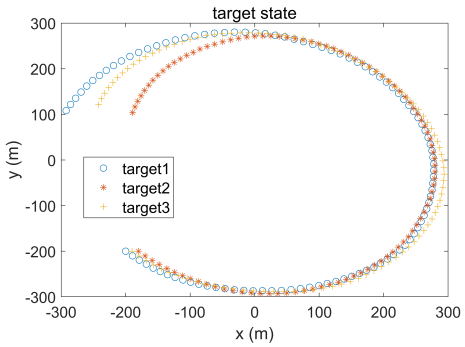

Fig. 1 Trajectories of the targets.

Suppose each agent carries one radar sensor and one or zero infrared sensor, and there are 5 infrared sensors in the system, i.e. $V_1 = \{1, ..., 10\}$, $V_2 = \{11, 12, 13\}$,

$M_1 = 5,\ M = 10,\ D_1 = \{1, ..., 10\},\ D_2 = \{11, ..., 15\}$. The state of sensor i at time instant k is $X_k^i = [A_k^i, B_k^i, \dot{A}_k^i, \dot{B}_k^i]^T,\ i \in D_1 \cup D_2$. A_k^i, B_k^i and $\dot{A}_k^i$, $\dot{B}_k^i$ are the position and velocity of sensor i in the direction of X and Y, respectively. The measuring model of sensor i is depicted as

$$\begin{aligned} y_{k,s}^i &= h^i(x_{k,s}) + v_k^i \\ &= \begin{cases} \begin{bmatrix} \sqrt{(A_k^i - a_{k,s})^2 + (B_k^i - b_{k,s})^2} \\ \arctan((B_k^i - b_{k,s})/(A_k^i - a_{k,s})) \end{bmatrix} + v_k^i, i \in D_1 \\ \arctan((B_k^i - b_{k,s})/(A_k^i - a_{k,s})) + v_k^i, i \in D_2\ . \end{cases} \end{aligned}$$

Since the infrared sensor is more accurate in angle measuring than radar sensor, one gets

$$Q_k^i = \begin{cases} \text{diag}(1, \pi/180), i \in D_1 \\ 0.2\pi/180, i \in D_2\ . \end{cases}$$

The state dynamics of each agent is taken by (26) with $B = \left[\begin{smallmatrix} 0 & -1 & 0 & 0 \\ 1 & 0 & 0 & 0 \end{smallmatrix}\right]^T$, $n_{k-1}^c = 0,\ c = 1, 2, ..., 10,\ g_k^c = [30 \sin \frac{(c-1)\pi}{5}, 30 \sin \frac{(c-1)\pi}{5}, 0, 0]^T,\ K = \left[\begin{smallmatrix} 0.0000 & & \\ -0.0550 & & \\ 0.0550 & 0.0014 & -0.0548 \\ 0.0000 & -0.0547 & -0.0043 \end{smallmatrix}\right]$ with initial states $[-150, -150, 10, 10]^T$. Suppose the directed interaction topology of the mutiagent systems $c \in V_1$ and multitarget $s \in V_2$ is as shown in Fig. 2.

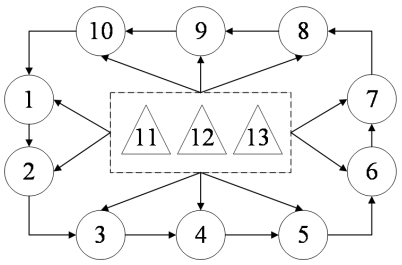

Fig. 2 Directed interaction topology.

The number of iterations L is chosen to be 100, and $MC = 50$ independent Monte Carlo simulations are performed to compare the average estimation errors $\left\{ \frac{1}{MC} \sum_{\eta=1}^{MC} [\| \hat{x}_{k|\eta}^i - x_{k|\eta} \|^2] \right\}^{1/2}$ of the MT-CKF algorithm proposed in this paper with the max-consensus algorithm and the centralized CKF algorithm,

where $\hat{x}^i_{k|\eta}$ and $x_{k|\eta}$ are the estimated and true states at the ηth Monte Carlo simulations, respectively. The average estimation errors are shown in Fig. 3. Fig. 3 shows that when $L = 100$, the boundness of all three algorithms are guaranteed and the performance of MT-CKF algorithm proposed in this paper is superior compared with the performance of max-consensus algorithm proposed in [31].

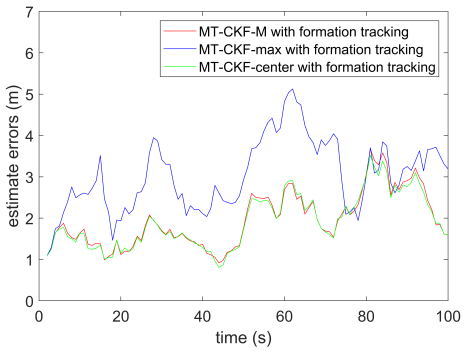

Fig. 3 State estimation errors with formation tracking.

Fig. 4 shows the state estimations and state estimation errors obtained by the proposed algorithm within one sensing period after several iterations, respectively. Obviously, the formation can estimate the states of multi-target with the bounded estimation errors, and the state estimations and the state estimation errors can achieve consistent at the current accuracy after about 90 iterations, respectively.

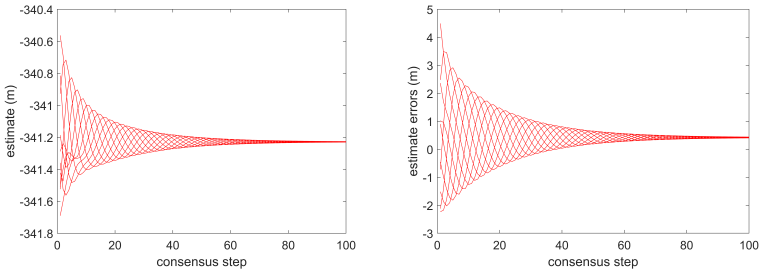

Fig. 4 (a) state estimation; (b) state estimation errors.

Fig. 5 shows the states of multi-agent systems, the state estimations of multi-target and the convex combination of the real states and the state estimations of multi-target at $t = 20s, 40s, 60s, 80s$, which are marked as '$\square$', '$\bigcirc$', '$*$', '$+$', respectively. Obviously, the convex combination of state estimations is close to that of the real states of multi-target, and agents make up a time-varying formation surrounding multi-target.

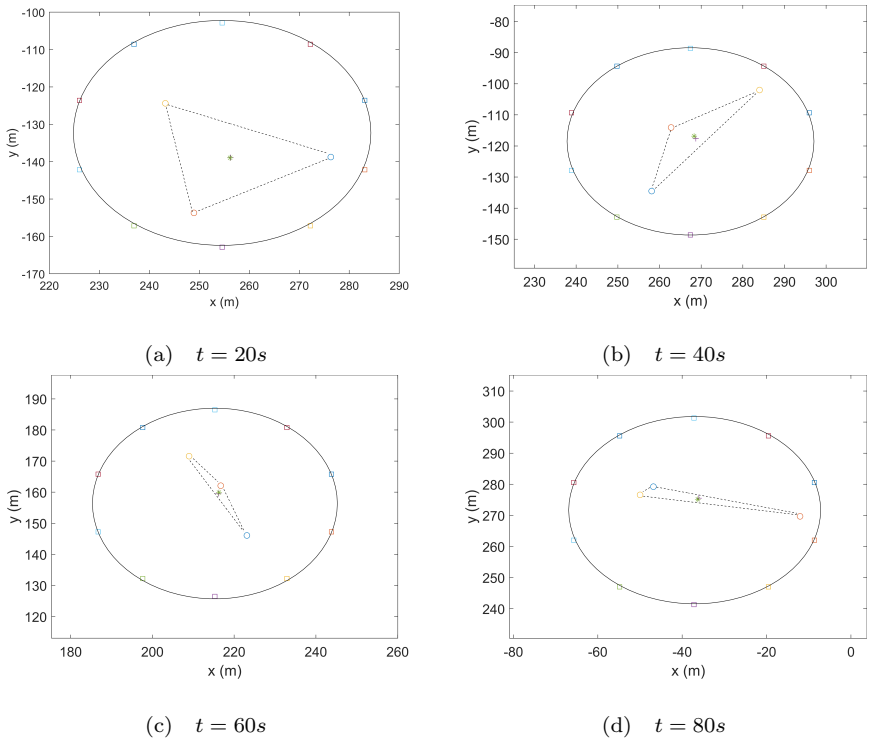

(a) $t = 20s$ (b) $t = 40s$

(c) $t = 60s$ (d) $t = 80s$

Fig. 5 Four time instants of multi-agent systems and multi-target.

The formation tracking errors $\| X_k^c - g_k^c - \sum_{s=M+1}^{N} (\frac{b_s}{\sum_{j=M+1}^{N} b_j} \hat{x}_{k,s})\|^2$, $c \in V_1$, $s \in V_2$ are shown in Fig. 6. Obviously, the boundedness of $\lim_{k \to +\infty} E(\| X_k^c - g_k^c - \sum_{s=M+1}^{N} (\frac{b_s}{\sum_{j=M+1}^{N} b_j} \hat{x}_{k,s})\|^2)$ is guaranteed.

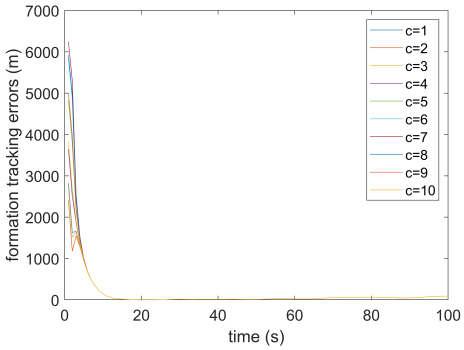

Fig. 6 The formation tracking errors.

6. Conclusion

A distributed MT-CKF algorithm based on the CKF scheme and heterogeneous sensors for multi-sensor multi-target filtering systems was proposed in this paper. Then a time-varying formation tracking protocol for multi-agent systems with multi-target using the distributed MT-CKF algorithm was designed. The state estimation errors and the formation tracking errors were proved to be bounded, and the formation tracking errors were increasing with the state estimation errors of the distributed MT-CKF algorithm and the errors generated in modeling the state dynamics of multi-target.

Foundation

This work was supported by the Science and Technology Innovation 2030-Key Project of "New Generation Artificial Intelligence" under Grant 2020AAA0-108200, the National Natural Science Foundation of China under Grants 62103016, 61922008, 62103023, 61973013, 61873011.

References

[1] L Wang, H He, Z Zeng, M F Ge, "Model-independent formation tracking of multiple Euler-Lagrange systems via bounded inputs," IEEE Transactions on Cybernetics, vol. 51, no. 5, pp. 2813-2823, May. 2021.

[2] T Y Xiong, Z Gu, "Observer-based adaptive fixed-time formation control for multi-agent systems with unknown uncertainties," Neurocomputing, vol. 423, pp. 506-517, Jan. 2021.

[3] Y Yuan, Y Wang, L Guo, "Sliding-mode-observer-based time-varying formation tracking for multispacecrafts subjected to switching topologies and time-delays," IEEE Transactions on Automatic Control, vol. 66, no. 8, pp. 3848-3855, Aug. 2021.

[4] R W Liao, L Han, X W Dong, Q D Li, Z Ren, "Finite-time formation-containment tracking for second-order multi-agent systems with a virtual leader of fully unknown input," Neurocomputing, vol. 415, pp. 234-246, Nov. 2020.

[5] T Y Xiong, Z Gu, "Observer-based adaptive fixed-time formation control for multi-agent systems with unknown uncertainties," vol. 423, pp. 506-517, Nov. 2021.

[6] X W Dong, "Formation and containment control for high-order linear swarm systems," Berlin, Germany: Springer-Verlag, pp. 36-43, 2015.

[7] R H Zheng, Y H Liu, D Sun, "Enclosing a target by nonholonomic mobile robots with bearing-only measurements", Automatica, vol. 53, pp. 400-407, Mar. 2015.

[8] B Pratama, A Muis, A Subiantoro, "Improved distributed formation control and trajectory tracking of multi quadrotor in leader-follower formation," 2019 5th International Conference on New Media Studies, pp. 129-134, Oct. 2019.

[9] R Ringback, J Wei, E S Erstorp, J Kuttenkeuler, T A. Johansen, K H Johansson, "Multi-agent formation tracking for autonomous surface vehicles," IEEE Transactions on Control Systems Technology, vol. 29, no. 6, pp. 2287-2298, Nov. 2021.

[10] H Liu, D Liu, Y Lyu, "Completely distributed time-varying formation target tracking for quadrotor team via image-based visual servoing," IEEE Transactions on Vehicular Technology, vol. 71, no. 1, pp. 21-32, Jan. 2022.

[11] X W Dong, Q K Tan, Q D Li, "Necessary and sufficient conditions for average formation tracking of second-order multi-agent systems with multiple leaders," Journal of the Franklin Institute, vol. 354, no. 2, pp. 611-626, Jan. 2017.

[12] X W Dong, G Q Hu. "Time-varying formation tracking for linear multi-agent systems with multiple leaders," IEEE Transactions on Automatic Control, vol. 62, no. 7, pp. 3658-3664, Jul. 2017.

[13] J Y Hu, P Bhowmick, A Lanzon. "Distributed adaptive time-varying group formation tracking for multi-agent systems with multiple leaders on directed graphs," IEEE Transactions on Control of Network Systems, vol. 7, no. 1, pp. 140-150, Mar. 2020.

[14] J L Yu, X W Dong, Z Ren, "Fully adaptive practical time-varying output formation tracking for high-order nonlinear stochastic multi-agent system with multiple leaders," IEEE Transactions on Cybernetics, vol. 51, no. 4, pp. 2265-2277, Apr. 2021.

[15] S He, H S Shin, A Tsourdos, "Distributed joint probabilistic data association filter with hybrid fusion strategy," IEEE Transactions on Instrumentation and Measurement, vol. 69, no. 1, pp. 286-300, Jan. 2020.

[16] H W Tian, Z L Jing, "A multi-space data association algorithm for target tracking systems," Communications in Nonlinear Science and Numerical Simulation, vol. 12, no. 4, pp. 608-617, Jul. 2007.

[17] C Z Qu, Y Zhang, X Zhang, Y Yang, "Reinforcement Learning-Based Data Association for Multiple Target Tracking in Clutter," Sensors, vol. 20, no. 22, Nov. 2020.

[18] M D Mustafa, N F Nabila, D J Evans, M Y Saman, A Mamat, "Association rules on significant rare data using second support," International Journal of Computer Mathematics, vol. 83, no. 1, pp. 69-80, Jan. 2006.

[19] T Ran, L Yuan, J Zhang, L He, R Huang, J Mei, "Not only look but infer: multiple hypothesis clustering of data association inference for semantic SLAM," IEEE Transactions on Instrumentation and Measurement, vol. 70, pp. 1-9, Jul, 2021.

[20] R P Mahler, "Random set theory for target tracking and identification", BocaRaton FL: CRC press, 2001.

[21] B T Vo, B N Vo and A Cantoni, "Bayesian filtering with random finite set observations," IEEE Transactions on Signal Processing, vol. 56, no. 4, pp. 1313-1326, Apr. 2008.

[22] G Battistelli, L Chisci, C Fantacci, "Consensus CPHD filter for distributed multitarget tracking," IEEE Journal of Selected Topics in Signal Processing, vol. 7, no. 3, pp. 508-520, Jun. 2013.

[23] W Yi, G Li, G Battistelli, "Distributed multi-sensor fusion of PHD filters with different sensor fields of view," IEEE Transactions on Signal Processing, vol. 68, pp. 5204-5218, Sep. 2020.

[24] D C Dalwadi, H B Soni, "A novel channel estimation technique of MIMO-OFDM system based on Extended Kalman filter," 2017 4th International Conference on Electronics and Communication Systems, pp. 158-163, Feb. 2017.

[25] G Zhang, "An improved UKF algorithm for extracting weak signals based on RBF neural network," IEEE Transactions on Instrumentation and Measurement, vol. 71, pp. 1-14, Jul. 2022.

[26] Z Wang, Y Huang, M Wang, J Wu, Y Zhang, "A computationally efficient outlier-robust cubature Kalman filter for underwater gravity matching navigation," IEEE Transactions on Instrumentation and Measurement, vol. 71, pp. 1-18, Jan. 2022.

[27] M Kooshkbaghi, H J Marquez, "Event-triggered discrete-time cubature Kalman filter for nonlinear dynamical systems with packet dropout," IEEE Transactions on Automatic Control, vol. 65, no. 5, pp. 2278-2285, Oct. 2019.

[28] B Manavoglu, "Target tracking with passive sensors using CKF," 2018 26th Signal Processing and Communications Applications Conference, pp. 1-4, May. 2018.

[29] Z Zhang, Q Li, L Han, X Dong, Y Liang , Z Ren, "Consensus Based Strong Tracking Adaptive Cubature Kalman Filtering for Nonlinear System Distributed Estimation," IEEE Access, vol. 7, pp. 98820-98831, Jul. 2019.

[30] L Tian, X W Dong, Q L Zhao, Q D Li, J H Lv, Z Ren, "Distributed adaptive time varying output formation tracking for heterogeneous swarm systems," Acta Automatica Sinica, vol. 47, no. 10, pp. 2386-2401, Oct. 2021.

[31] Y Zhang, L Sun, G Hu, "Distributed consensus-based multitarget filtering and its application in formation-containment control," IEEE Transactions on Control of Network Systems, vol. 7, no. 1, pp. 503-515, Mar. 2020.

[32] T R Wanasinghe, G K I Mann, R G Gosine, "Stability analysis of the discrete-time cubature Kalman filter," 2015 54th IEEE Conference on Decision and Control, pp. 5031-5036, Dec. 2015.

[33] G Battistelli, L Chisci, "Kullback-Leibler average, consensus on probability densities, and distributed state estimation with guaranteed stability," Automatica, vol. 50, no. 3, pp. 707-718, Mar. 2014.

[34] W Song, J Wang, S Zhao, J Shan, "Event-triggered cooperative unscented kalman filtering and its application in multi-uav systems," Automatica, vol. 105, pp. 264-273, Jul. 2019.

[35] J Shi, G Qi, Y Li, A Sheng, "Stochastic convergence analysis of cubature Kalman filter with intermittent observations," Journal of Systems Engineering and Electronics, vol. 29, no. 4, 823-833, Aug. 2018.